

RSC Advances



This is an *Accepted Manuscript*, which has been through the Royal Society of Chemistry peer review process and has been accepted for publication.

Accepted Manuscripts are published online shortly after acceptance, before technical editing, formatting and proof reading. Using this free service, authors can make their results available to the community, in citable form, before we publish the edited article. This *Accepted Manuscript* will be replaced by the edited, formatted and paginated article as soon as this is available.

You can find more information about *Accepted Manuscripts* in the [Information for Authors](#).

Please note that technical editing may introduce minor changes to the text and/or graphics, which may alter content. The journal's standard [Terms & Conditions](#) and the [Ethical guidelines](#) still apply. In no event shall the Royal Society of Chemistry be held responsible for any errors or omissions in this *Accepted Manuscript* or any consequences arising from the use of any information it contains.



ARTICLE

Fabrication of titanium dioxide with durable superhydrophilicity by anodization

Received 00th June 20xx,
Accepted 00th June 20xx

DOI: 10.1039/x0xx00000x

www.rsc.org/

Zhaoguo Zhang, Xudong Cheng, Zhengfeng Huang, Qingli Wang, Peimei Dong, Yi Chen and Xiwen Zhang*

Titanium-based materials with specific wettability show promising potential applications. In this paper, titanium plate with hydrophilicity was simply synthesized by anodization with the electrolyte composed of NaOH, and their durability of wettability in the air was evaluated. The properties of the anodized Ti plate were characterized by a series of tests including FESEM, roughness, BET surface area, XRD, XPS, water contact angle, UV-vis absorption, photoluminescence, photocatalytic decomposition ability of methylene blue, self-cleaning property and durability of wettability in the air. When the processing time of the anodization was 10 minutes, the resulting titanium plate had a water contact angle of 0°, which proved it to be superhydrophilic, and it possessed a micro-nano composite architecture with a distinct nanofiber network chemically constituted of anatase and sodium titanate. It also exhibited excellent photocatalytic properties under UV illumination, including high photocatalytic activity and photocatalytic decomposition ability, as well as good self-cleaning property, all of which rendered it to have good durability of wettability. Significantly, it can maintain the superhydrophilicity for 6 months in the air. It is proposed that it is a synergy effect originating from the topology, chemical constitution and excellent photocatalytic properties that leads to the durable superhydrophilicity.

Introduction

As one of the most important properties of a material, the wettability of its surface has a significant influence on its potential applicable domains.¹⁻⁷ From the pioneering works of Wenzel and Cassie et al,^{8, 9} the relationship between the topology structure and the wettability of its surface was thoroughly investigated, theoretically demonstrating that the topology structure plays a crucial role on the wettability of the surface. Combined with the fundamental effect of surface chemical composition on wettability, it is possible to manufacture a material with a surface possessing expected degree of wettability,¹⁰ for example, the superhydrophilic surface. Generally, a superhydrophilic surface refers to a surface whose water contact angle is less than 5°, and it has been previously proven that the superhydrophilic surface exhibits desirable properties such as self-cleaning and antifouling.¹¹

Titanium (Ti) has been widely utilized in fields such as the cooling system of nuclear power plants due to its prominent mechanical properties and corrosion resistance.¹² Undoubtedly, the thermal exchange efficiency can be remarkably elevated by a more sufficient contact between the hot liquid and hydrophilic Ti surface.¹³ Efforts have been

devoted to the synthesis of Ti-based materials with hydrophilic surfaces.^{14, 15} Presently, Ti-based materials with hydrophilic surfaces are mainly produced according to typical thought which consists of two aspects; one is the construction of roughened surface by chemical or mechanical methods, and the other is the formation of hydrophilic substances. Owing to features like easy manipulation and low cost, electrochemical anodization is a prevalent technique in treating Ti materials to obtain hydrophilic surfaces. Ottone et al fabricated hydrophilic TiO₂ nanotubes on a commercial pure titanium foil via an anodic oxidation, which had a water contact angle of about 28°. Lan et al obtained TiO₂ nanotubes through a self-ordering process during the anodic oxidation treatment, and the resulting TiO₂ nanotubes with different diameters showed a diameter-sensitive hydrophilicity.¹⁷ Li et al fabricated hierarchical TiO₂ nanotubes on the surface of porous Ti foil by an electrochemical treatment; after a following calcination in the air, the resulting surface showed a water contact angle of approximately 0°, proven to be superhydrophilic.¹⁸ Another crucial issue is the durability of the surface wettability under a certain environment, reflecting the ability of a surface to retain its feature of wettability, which has a great impact on its practical application value. The durability of surface wettability is a complex issue, which involves aspects including the intrinsic properties of the surface and the exposed environment.¹⁹⁻²¹ In practical applications, a surface easily loses its original wettability from the contamination of adsorbed molecules such as organics. In terms of superhydrophilic surface, such TiO₂-related materials with

Address: School of Materials Science and Engineering, Zhejiang University, Hangzhou, 310027, People's Republic of China

*Corresponding Author: Tel.: +86 571 88276234; Fax: +86 571 87952341; E-mail: zhangxw@zju.edu.cn

hydrophilic surfaces are usually preserved in a solution to maintain their hydrophilicity, from which any dissolved oxygen has been removed in advance. In the presence of water, the contaminants on TiO₂-related materials can be photocatalytically decomposed under light irradiation by photo-generated oxidative holes and hydroxyl groups. Recently, the reservation of the superhydrophilicity can be realized by either adding additives to TiO₂, such as SiO₂, or providing intermittent UV irradiation.^{22, 23} Machida et. al. prepared the 12·SiO₂-88·TiO₂ mol% composite film, after one week of exposure in the air, its water contact angle arose from 0° to 9.6°, failing to maintain its superhydrophilicity.²² When superhydrophilic TiO₂ is prepared *in situ* on a Ti metal substrate by methods such as anodization, the treated Ti-based material is functionalized and yields desirable properties including antifouling and self-cleaning abilities without obvious change of the original mechanical properties, which largely elevates the possibility of obtaining a durable superhydrophilicity. In addition, compared with the conventional free-standing TiO₂ photocatalysts such as P25 TiO₂ powders, the anodized TiO₂ can well resolve the tough issues such as hard to recycle and easy to agglomerate.²⁴ However, to the best of our knowledge, there is no report concerning the preparation of Ti-based materials with durable superhydrophilicity via employing a facile one-step anodization treatment without further modification.

Herein, the superhydrophilic Ti plate with durability in the air is prepared by a one-step anodization using 4M NaOH solution as the electrolyte. The durable superhydrophilicity of the resulting anodized Ti plate can be attributed to the synergy effect of the following aspects: the micro-nano composite architecture consisting of micro-scale pit-like structures and a nanofiber network; the surface chemical constitution including anatase and sodium titanate; the excellent photocatalytic activity; the relatively high photocatalytic decomposition ability and the self-cleaning ability. This paper provides a facile method to synthesize Ti-based materials with superhydrophilic surfaces, furthermore, it promotes understanding of the durability of hydrophilicity.

Experimental

Materials

Ti plate (TA0) was provided by Baotai Group (China). Acetone (AR), nitric acid (HNO₃, AR), hydrofluoric acid (HF, AR), hydrochloric acid (HCl, AR), sodium hydrate (NaOH, AR) and methylene blue (MB) were purchased from the Sinopharm Chemical Reagent Co., Ltd. P25 TiO₂ powders were produced by Degussa Co., Germany. n-dodecyltrimethoxysilane (nD) was supplied by Alfa Aesar. Deionized water (DI) was used in the whole process.

Synthesis of samples

The polished Ti plates (2cm × 4cm) were thoroughly rinsed with DI, acetone and DI sequentially to remove the contaminants on the surface, followed by an acid-washing treatment with the mixed solution consisting of HF, HNO₃ and

DI at a volume ratio of 1:1:1. A Ti plate, as the anode, was then placed into a polypropylene reactor containing 4M NaOH solution, with a parallel Pt plate functioning as the cathode which was situated 8cm away from the Ti plate. The anodization treatment was carried out on electrochemical work station (ES550, Gauss Union Technology Co., Ltd., China) with a 10V DC voltage at 25 °C for different processing times, and the as-prepared anodized Ti plates were accordingly labeled as AT-X, with AT-5 as the designation for the sample with a processing time of 5 minutes, and AT-10 for a processing time of 10 minutes. When finished, the resulting Ti plates were purged by DI, and then immersed into a diluted HCl solution (0.05M) for 1 hour. Finally, the anodized Ti plates were purged using DI, and dried in the air.

Characterization

Morphologies of the as-prepared samples were obtained by a field emission scanning electron microscope (FESEM, Hitachi S4800) equipped with an energy dispersive X-ray detector (EDS). Specific surface areas of the resultant anodized Ti plates were determined by nitrogen adsorption at 77 K with the Brunauer-Emmett-Teller (BET) method on a gas adsorption apparatus (AUTOSORB-1-C, Quantachrome Instruments). The roughnesses of the resulting samples were measured employing a surface roughness measuring instrument (HOMMEL-ETAMIC W10, Germany). X-ray diffraction (XRD) patterns of the anodized Ti plates were recorded on a PANalytical X'Pert PRO X-ray diffractometer using Cu K α radiation with a 2 θ scan range from 20° to 80° at a rate of 4 °/min. X-ray photoelectron spectroscopy (XPS) measurements of sample AT-10 were conducted utilizing a VG ESCALAB MARK II spectrometer with an Mg K α (1253.6 eV) X-ray source.

Measurement of photocatalytic activity

UV-vis absorption spectra of the anodized Ti plates were measured on a UV-2600 UV-vis spectrophotometer (Shimadzu Corporation) using a 350 nm excitation wavelength at room temperature. Photoluminescence spectra (PL) of the anodized Ti plates were carried out on a FLS920 fluorescence spectrometer (Edinburgh Instruments Ltd.) at room temperature using 320 nm as an excitation wavelength. The evaluations of the photocatalytic decomposition abilities of the resulting samples were executed on a UV-2600 UV-vis spectrophotometer (Shimadzu Corporation) via a series of 3-hour photocatalytic degradations of MB (10 mM aqueous solution) under UV illumination of 10 mW/cm². In order to investigate the adsorption capacity for MB on the surface of as-prepared samples and P25 TiO₂ powders, the catalysts were placed in the MB aqueous (10 μ M) in the absence of light for 3 hours to obtain the adsorption behaviour on the surface. After every 30 minutes illumination time, the MB concentration was measured. According to the adsorption results, the decomposition of MB were corrected.

Self-cleaning property

As a model contaminant, n-dodecyltrimethoxysilane (nD) was chosen to contaminate the as-prepared anodized Ti plates, and the self-cleaning properties of the anodized Ti plates were accordingly examined by measuring the variations of water

contact angle of the above nD-contaminated samples in the presence of successive UV illumination.

Measurement of the durability of wettability

Water contact angles of the samples exposed in the air were measured once a month by a video-based contact angle measuring device (OCA 20, Dataphysics Instruments GmbH, Germany) at ambient temperature, and the 6-month duration results were used to characterize the durability of wettability.

Results and discussion

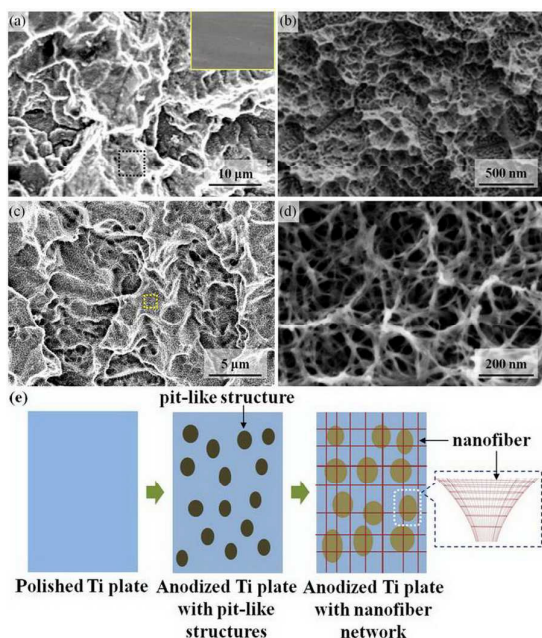


Fig. 1 (a) - (d) FESEM images of the as-prepared anodized Ti plates, (a) and (b) AT-5, (c) and (d) AT-10; inset of (a) the polished Ti plate before anodization. (e) Schematic representation of formation mechanism of Ti plate with micro-nano composite architecture by anodization.

Fig. 1 shows the FESEM images of the resulting Ti plates after anodization. Obviously, compared with the smooth polished Ti plate (inset of Fig. 1a), the surface of the anodized Ti plate became roughened, and, moreover, the topology varied depending on the processing time of anodization. As shown in Fig. 1a, the sample AT-5 was preliminarily etched and obtained micro-scale pit-like structures with sizes ranging from several to tens of micrometers.²⁵ For a randomly selected zone, it is evident that the above micro-scale structures were actually composed of smaller adjacent pit-like structures with sizes of about 200 ~ 400 nm (Fig. 1b). Thus, the sample AT-5 had a nested topology consisting of micro-scale and nano-scale pit-like structures. As previously reported, the anodization of Ti initially starts in the form of point-etching;^{26, 27} given the fact that the OH⁻ concentration dramatically decreases from the bottom to the mouth of the pit-like structure, as well as the effects of heat and current, the etching rate also drops sharply from the bottom to the mouth of the pit-like structure. Thus, the local etching rate in the bottom is far larger than that in

the mouth.²⁸⁻³⁰ Hence, once such etching spots form, the etching process proceeds longitudinally to the interior to form new smaller pit-like structures, while also proceeding laterally to etch the walls of the pit-like structures. When the processing time was 10 minutes, an ambiguous new structure emerged in the sample AT-10 because of the further etching of the aforementioned structures (Fig. 1c). The observation of the selected zone clearly shows the presence of a nanofiber network covering the entire surface and stretching to the interior (Fig. 1d). The nanofiber network resulted from the etching which crossed the walls of pit-like structures. The network was composed of interconnected fibers whose sizes ranged from ten to forty nanometers, and the intervals between nanofibers were about 200 nm, which greatly augments the porosity. Thus, the surface of AT-10 formed a finer micro-nano composite architecture comprised of micro-scale pit-like structures and a nanofiber network. Consequently, when treated by anodization, the surface of Ti plate becomes roughened, accompanied by the formation of micro-nano pit-like structures. With appropriate increase of the processing time, the anodized Ti plate eventually accomplishes a fine micro-nano composite architecture which consists of micro-nano pit-like structures and a nanofiber network (Fig. 1e). It is important to point out that the formation of a micro-nano composite architecture is beneficial to the enhancement of the hydrophilicity.

Table 1 BET surface areas and roughness of the as-prepared anodized Ti plates, AT-5 and AT-10.

Sample	BET surface area (m ² /g)	Roughness (μm)
AT-5	52	0.87
Ho-TiO ₂	548	1.53

Table 1 shows the BET surface areas and roughness of the as-prepared anodized Ti plates. AT-5 exhibited a BET surface area of 52 m²/g and a roughness of 0.87 μm, and AT-10 showed a BET surface area of 548 m²/g and a roughness of 1.53 μm. Apparently, both the BET surface area and roughness are significantly augmented with the increase of the processing time. It is notable that the BET surface area of AT-10 is increased by 9.5 times in comparison with that of AT-5, and such an enormous increase is mainly induced by the existence of the nanofiber network. These data support well the above FESEM results to accurately reflect the topology.

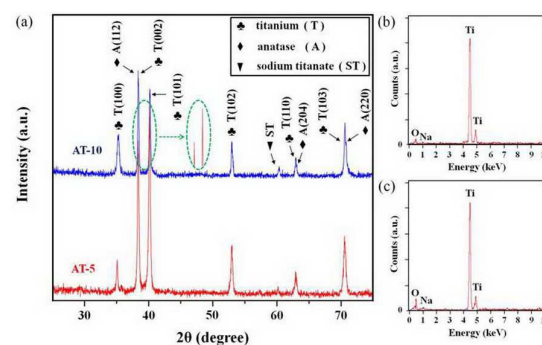


Fig. 2 (a) XRD patterns of the prepared anodized Ti plates: (■) AT-5, (■) AT-10; corresponding EDS spectra (b) AT-5, (c) AT-10.

ARTICLE

RSC Advances

In order to study the crystallization of the resulting anodized Ti plates, the XRD patterns and EDS spectra were obtained, as shown in Fig. 2. During the anodization process, TiO_2 and sodium titanate are produced by the reaction of Ti with the electrolyte (reaction 1 in Table 2). From the following washing treatment with 0.05M HCl solution, partial sodium titanate undergoes an ion exchange reaction and turns into anatase after drying in the air (reactions 2 and 3 in Table 2). Owing to the influence of the substrate, the intensities of the Ti peaks are strong in both samples.^{31,32} As some of the TiO_2 peaks are close to the Ti peaks, it is necessary to strictly separate them. The peak intensities in the XRD pattern of AT-10 generally declined; relative to those of AT-5 when comparing the intensity ratio of peaks centred at 38.5° and 40.4° ; this discrepancy suggests the presence of anatase (112) in AT-10. The anatase (204) and (220) peaks were also detected, as well as sodium titanate centred at about 61.2° . Thus, the anodized Ti plates possessed peaks which can be assigned to the Ti-containing phases such as anatase and sodium titanate other than the major Ti phase (Fig. 2a).³³ The presence of the O and Na elements in the EDS spectra can also manifest the formation of these newly-formed Ti-containing phases (Fig. 2b and c). Clearly, the content of TiO_2 is remarkably increased with the corresponding extent of the anodization. Considering the fact that the Ti peak intensity of AT-10 is more susceptible to the substrate due to its distinct topology, it is certain that the contents of sodium titanate and anatase are actually higher than their apparent intensities in the XRD pattern indicate. As anatase is not only hydrophilic but also possesses photocatalytic activity, the increase of anatase content can be beneficial to the enhancement of the hydrophilicity and photocatalytic activity of the anodized Ti plate.

Table 2 Reactions during the synthesis of samples by anodization.

	Reaction
(1)	$3\text{Ti} + 2\text{NaOH} + 5\text{H}_2\text{O} \rightarrow \text{Na}_2\text{Ti}_3\text{O}_7 + 6\text{H}_2 \uparrow$
(2)	$\text{Na}_2\text{Ti}_3\text{O}_7 + x\text{H}^+ \rightarrow \text{Na}_{2-x}\text{H}_x\text{Ti}_3\text{O}_7 + x\text{Na}^+$
(3)	$\text{H}_2\text{Ti}_3\text{O}_7 \rightarrow 3\text{TiO}_2 + \text{H}_2\text{O}$

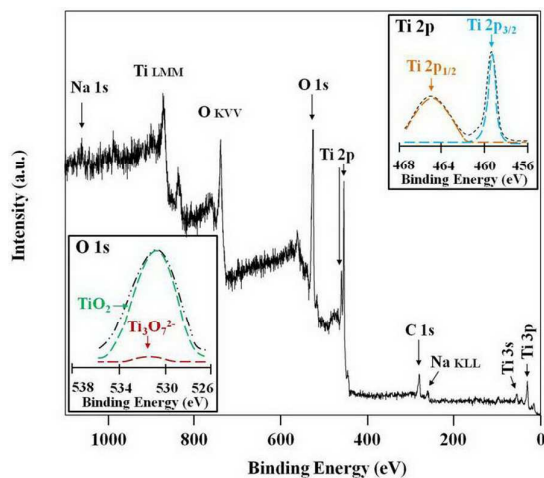


Fig. 3 XPS survey spectrum of the sample AT-10; insets are corresponding high-resolution XPS spectra, the top right corner for Ti 2p (the Gaussian

fitting curves are colored), the bottom left corner for O 1s (the Gaussian fitting curves are colored).

The XPS analysis was carried out to confirm the chemical constitution of the anodized Ti plates. Fig. 3 shows the XPS spectrum of AT-10, and peaks identified as Ti, O, Na and C are present. The C 1s peak at 284.6 eV can be ascribed to the carbon used as an energy reference in the XPS measurements.³⁴ To obtain more details, high-resolution XPS measurements were executed, and the resulting spectra for Ti 2p and O 1s are depicted in the insets of Fig. 3. For the Ti 2p spectrum, peaks centered at 458.6 eV and 464.4 eV were observed, which were assigned to the Ti 2p_{3/2} and Ti 2p_{1/2} respectively.²⁷ The interval between the Ti 2p_{3/2} and Ti 2p_{1/2} peaks was 5.8 eV, slightly larger than that of the pure TiO_2 , which resulted from the Ti in the $\text{Ti}_3\text{O}_7^{2-}$ group. The O 1s peak was deconvoluted into two Gaussian fitting curves situated at 530.5 eV and 531.8 eV,^{27,31} which were assigned to the oxygen in TiO_2 and $\text{Ti}_3\text{O}_7^{2-}$ group, respectively. Thus, the presence of sodium titanate and TiO_2 can be confirmed, which is in agreement with the above XRD and EDS results. Furthermore, based on the XPS data, the atomic ratio of AT-10 was roughly calculated, and the chemical constitution was determined at a TiO_2 :sodium titanate ratio of 49:1, indicating that TiO_2 was the phase with the absolute majority in the products.

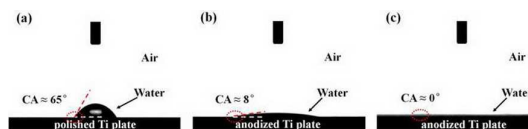


Fig. 4 Water contact angles of (a) the polished Ti plate before anodization treatment; anodized Ti plates: (b) AT-5, (c) AT-10.

To determine the wettability of the as-prepared anodized Ti plates, measurements of water contact angles were implemented, and the corresponding images of the water contact angles are presented in Fig. 4. As shown in Fig. 4a, the polished Ti plate had a water contact angle of 65° . After anodization treatment, the water contact angles were dramatically decreased, which resulted from the increase of surface roughness and the existence of hydrophilic substances including anatase and sodium titanate.³⁵ The water contact angle of AT-5 was 8° (Fig. 4b); meanwhile, AT-10 had a water contact angle of approximately 0° (Fig. 4c), being superhydrophilic. Compared with AT-5, AT-10 possesses a distinct nanofiber network structure, which is extremely crucial for its superhydrophilicity.¹⁸ The wetting process of AT-10 can be elucidated as follows: on contact with the surface, water spreads fast along the external hydrophilic nanofibers of the network, and the wetted nanofibers promote the invasion of water to the interior by gravity. By this layer-by-layer mode, air is completely exhausted through the interconnected network, and water eventually fills the pores of the network.

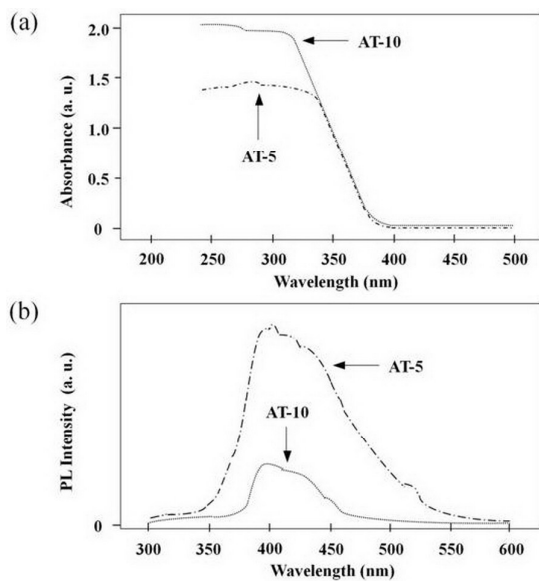


Fig. 5 (a) UV-vis absorption spectra and (b) photoluminescence spectra of the anodized Ti plates AT-5 and AT-10.

Fig. 5a exhibits the UV-vis absorption spectra of the as-prepared anodized Ti plates of AT-5 and AT-10. Compared with AT-5, AT-10 yielded a higher absorbance intensity in the UV region. Meanwhile, both AT-5 and AT-10 showed a comparable cutoff wavelength of about 387 nm. The same chemical constitution leads to a comparable band gap, while the higher BET surface area and content of anatase endowed the AT-10 with a better absorbance.³⁶ In addition, their photoluminescence (PL) spectra were measured to investigate the behaviour of photo-generated charge carriers, and the results are shown in Fig. 5b. On excitation by the incident light, photo-generated electron-hole pairs are present in TiO_2 , but they separate shortly after their formation to form sole electrons and holes. However, when the sole charge carrier encounters another charge carrier with inverse charge, a recombination of electron and hole will take place, leading to an increase of PL intensity. The PL spectra of AT-5 and AT-10 are similar, with a wide peak in the region of 395 ~ 450 nm, which was consistent with the PL spectrum of pure TiO_2 from previous reports. However, it is obvious that the PL intensity of AT-10 was far lower in comparison with that of AT-5, indicating that the recombination of photo-generated charge carriers was efficiently suppressed in AT-10. This observed difference in the PL spectra can be attributed to the presence of the representative nanofiber network in AT-10;³⁷ as the TiO_2 nanofibers can significantly promote the transfer of photo-generated charge carriers, the possibility of reaction between the sole charge carrier and species such as water is greatly augmented during the charge transfer process, thus the recombination of photo-generated charge carriers is retarded, resulting in a decrease of PL intensity. As aforementioned, AT-10 exhibits high absorbance intensity combined with relatively low PL intensity; consequently, it possesses good photocatalytic activity.

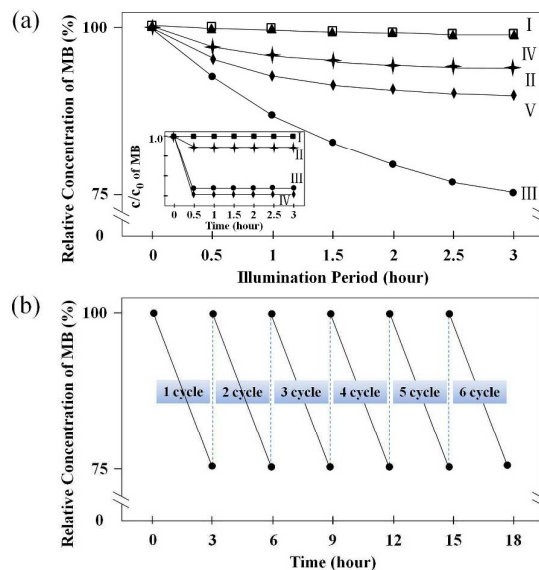


Fig. 6 (a) The variation of methylene blue (MB) relative concentration under different conditions with UV illumination, (I) polished Ti plate, (II) AT-5, (III) AT-10, (IV) free of Ti or anodized Ti plate, (V) P25 TiO_2 powders. (b) Photocatalytic activity of AT-10 for MB degradation over six degradation cycles with UV illumination. Inset of (a) is the adsorption behaviour of MB on (I) polished Ti plate, (II) AT-5, (III) AT-10, (IV) P25 TiO_2 powders.

Based on the photocatalytic activity, the photocatalytic decomposition performance of the prepared anodized Ti plates was evaluated by measuring the decomposition rate of MB under UV illumination at 25 °C, and the results are shown in Fig. 6a. It can be seen that the control groups, with polished Ti plate or free of Ti/anodized Ti plate, showed low decrease rates for the relative MB concentration (curve I and curve IV in Fig. 6a), and this slight decrease of the relative MB concentration resulted from the self-degradation of MB under UV illumination;¹⁹ on the contrary, the anodized Ti plates exhibited much higher decrease rates for the relative MB concentration (curve II and curve III in Fig. 6a), indicating that the presence of anodized Ti plate with photocatalytic activity can readily facilitate the decomposition of MB under UV illumination. Meanwhile, the P25 TiO_2 powders system (curve V in Fig. 6a) gave a MB decomposition rate of 3.4%/h. Given that the mass of P25 TiO_2 powders was apparently larger than the TiO_2 of AT-10, the ability of AT-10 was more than 2.5 times than that of the P25 TiO_2 powders. Taguchi et. al fabricated the anatase TiO_2 mesoporous film by anodizing titanium specimens with NaCl/ethylene glycol solution.³⁸ When the concentration of MB was 10 mM, the TiO_2 mesoporous film had a MB decomposition rate of 1.2 %/h under UV irradiation, which was approximately 1/7 fold of the same area of AT-10. The inset of Fig. 6a showed adsorption behavior of MB on the as-prepared samples and P25 TiO_2 powders. Clearly, AT-10 and P25 TiO_2 powders showed higher adsorption capacity for MB than that of AT-5, meanwhile, adsorption capacity for MB of AT-10 was slightly lower than that of the P25 TiO_2 powders, resulting from the considerable large amount of P25 TiO_2 powders. Notably, the adsorption of MB were far less than the initial concentration. A higher adsorption capacity for MB was

beneficial for the following photocatalytic decomposition of MB under illumination. The relative MB concentration of AT-5 decreased by 6% after 3-hour decomposition, while that of AT-10 decreased by 25%, an increase of by 3.2 fold. In addition, the decomposition reaction of MB obeyed pseudo-first-order kinetics, and the mean decrease rates of the relative concentration of MB were 2.0%/h and 8.2%/h for AT-5 and AT-10, respectively. Thus, AT-10 had a higher decomposition ability than AT-5, and the results can be explained by the following three aspects: (1) AT-10 had a higher BET surface area, which remarkably augmented the direct contact between MB and TiO₂ to favour the decomposition of the former; (2) AT-10 had better photocatalytic activity, as shown in the above UV absorption and PL spectra; (3) AT-10 possessed a micro-nano composite architecture with nanofiber network, which can greatly facilitate the utilization of incident light. Additionally, the stability of the photocatalytic decomposition ability of AT-10 was tested by carrying out a 6-cycle decomposition of MB under UV illumination, and the final concentration of MB of each cycle was determined, as presented in Fig. 6b. Obviously, as apparent in Fig. 6b, AT-10 exhibited a comparable, constant cycle-end concentration during the entire test, demonstrating a stable and consistently effective photocatalytic decomposition performance.

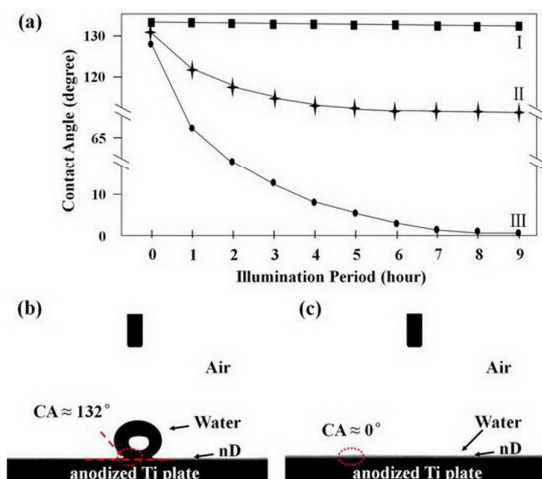


Fig. 7 (a) The evolution of the water contact angles of the *n*-dodecyltrimethoxysilane (nD)-contaminated samples with UV illumination time, (I) polished Ti plate, (II) AT-5, (III) AT-10. Water contact angles of AT-10 after (b) 0 h, (c) 9 h.

The surface of a material is easily polluted by contaminants such as organics when exposed to the ambient environment, which can have a great impact on the corresponding surface properties, especially the wettability.³⁹ It is well-known that a superhydrophilic surface shows a self-cleaning property, and the surface chemically constituted by substances possessing photocatalytic decomposition ability enhances the self-cleaning property. To investigate this property, the self-cleaning abilities of the prepared anodized Ti plates were assessed by measuring the variations of water contact angle of nD-contaminated samples under UV illumination (Fig. 7a). After contamination by nD, the water contact angles were

about 130° due to the loss of roughness and chemical constitution.^{18,19} As shown in the control group (curve I of Fig. 7a), there was no obvious change of the water contact angles of the polished Ti plate during the measurements, indicating that nD did not decompose in the presence of Ti under UV illumination. Compared with the polished Ti plate, the water contact angles of anodized Ti plate showed an apparent downward tendency. AT-5 attained a final water contact angle of about 90° (curve II of Fig. 7a). In contrast, the water contact angle of AT-10 gradually decreased from the initial value of 128° (Fig. 7b) to the final value of 0° (Fig. 7c), eventually restoring the superhydrophilicity. The restoration of the superhydrophilicity of AT-10 can be attributed to the complete removal of the surface-adsorbed nD molecules by direct decomposition using the oxidative photo-generated holes and hydroxyl radicals, that is, the photo-induced self-cleaning property.¹¹ The sample AT-10 with self-cleaning ability will thus maintain its surface properties for a longer period.

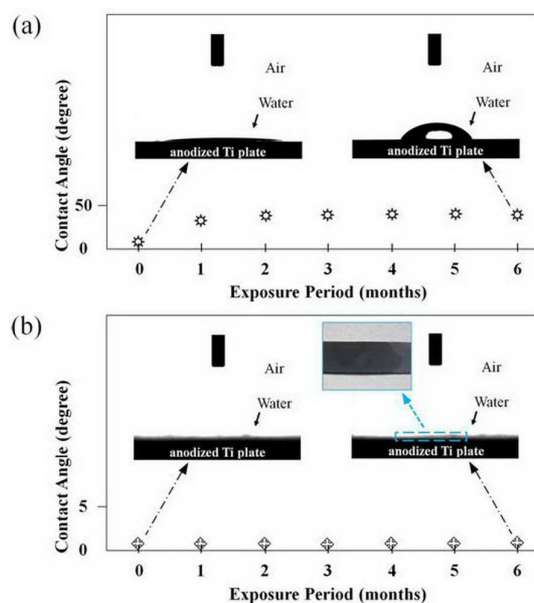


Fig. 8 The variations of water contact angles of the anodized Ti plates with exposure period in the air, (a) AT-5, (b) AT-10. The inset of (b) is a photograph showing the water mat on the surface of AT-10 with 6-month exposure to the air.

Aiming at characterizing the durability of wettability in the air, the water contact angles of anodized Ti plates were measured once a month, and the results are plotted in Fig. 8. Overall, the water contact angle variation curves showed different tendencies. For AT-5, the water contact angle dramatically increased in the first two months, from 8° to approximately 47°, and finally maintained a value at about 50° (Fig. 8a), indicating a bad durability of wettability. However, the water contact angles of AT-10 were comparable to the initial one during the whole test, and eventually stabilized at about 0° (Fig. 8b), showing an excellent durability of the superhydrophilicity in the air. Permpoon et. al. prepared the 20·SiO₂-80·TiO₂ mol% composite film with persistent superhydrophilicity. Then, only after two-week exposure in the air, the water contact angle of

the SiO₂-TiO₂ composite film had greatly augmented from 0 ° to 12 °, losing the superhydrophilicity.⁴⁰ During the measurement of AT-10 water contact angle, we observed that the water droplet spread quickly and formed a water mat on the surface after 6-month exposure in the air. The superior durability of superhydrophilicity of AT-10 is ascribed to the high self-cleaning ability originating from the photocatalytic decomposition ability and photocatalytic activity. Such Ti material with durable hydrophilicity makes great sense for a variety of practical applications.

Conclusions

Superhydrophilic Ti plate was synthesized by anodization. The anodized Ti plate formed a micro-nano composite architecture with a typical nanofiber network, and the chemical constitution was composed of anatase and a slight sodium titanate. This superhydrophilic surface exhibited high UV-vis absorbance and low PL intensity, showing good photocatalytic activity. Additionally, the surface also exhibited consistently effective photocatalytic decomposition in the degradation of MB under UV illumination. In particular, when nD was used as a model contaminant, the superhydrophilicity of the contaminated surface was restored after 9-hour UV illumination, demonstrating an excellent self-cleaning property. Notably, the surface can maintain the superhydrophilicity after 6-month exposure in the air, indicating desirable durability of wettability. It is assumed that the durable superhydrophilicity originates from a synergy effect between topology, chemical constitution, high photocatalytic activity, photocatalytic decomposition ability and self-cleaning property.

Acknowledgements

This work was supported by the Chinese National Natural Science Foundation (No. 50772098).

Notes and references

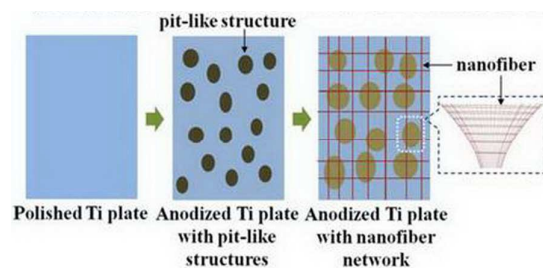
1. Y. Zhang, Y. Chen, L. Shi, J. Li and Z. Guo, *J. Mater. Chem.*, 2012, **22**, 799-815.
2. A. Marmur, *Soft Matter*, 2013, **9**, 7900-7904.
3. B. Wang, W. Liang, Z. Guo and W. Liu, *Chem. Soc. Rev.*, 2015, **44**, 336-361.
4. K. Liu and L. Jiang, *Nanoscale*, 2011, **3**, 825-838.
5. N. Gao and Y. Yan, *Nanoscale*, 2012, **4**, 2202-2218.
6. N. T. Chamakos, M. E. Kavousanakis and A. G. Papathanasiou, *Soft Matter*, 2013, **9**, 9624-9632.
7. S. Morgenthaler, C. Zink and N. D. Spencer, *Soft Matter*, 2008, **4**, 419-434.
8. R. N. Wenzel, *Ind. Eng. Chem.*, 1936, **28**, 988-994.
9. A. Cassie and S. Baxter, *Trans. Faraday Soc.*, 1944, **40**, 546-551.
10. T. Sun, L. Feng, X. Gao and L. Jiang, *Acc. Chem. Res.*, 2005, **38**, 644-652.
11. R. Wang, K. Hashimoto, A. Fujishima, M. Chikuni, E. Kojima, A. Kitamura, M. Shimohigoshi and T. Watanabe, *Nature*, 1997, **388**, 431-432.
12. J. Yong, F. Chen, Q. Yang, U. Farooq and X. Hou, *J. Mater. Chem. A*, 2015, **3**, 10703-10709.
13. Y. Takata, S. Hidaka, M. Masuda and T. Ito, *Int. J. Energy Res.*, 2003, **27**, 111-119.
14. S. Tugulu, K. Löwe, D. Scharnweber and F. Schlottig, *J. Mater. Sci.: Mater. Med.*, 2010, **21**, 2751-2763.
15. J. Liang, K. Liu, D. Wang, H. Li, P. Li, S. Li, S. Su, S. Xu and Y. Luo, *Appl. Surf. Sci.*, 2015, **338**, 126-136.
16. C. Ottone, A. Lamberti, M. Fontana and V. Cauda, *J. Electrochem. Soc.*, 2014, **161**, 484-488.
17. M. Lan, C. Liu, H. Huang, J. Chang and S. Lee, *Nanoscale Res. Lett.*, 2013, **8**, 150-157.
18. L. Li, Z. Liu, Q. Zhang, C. Meng, T. Zhang and J. Zhai, *J. Mater. Chem. A*, 2015, **3**, 1279-1286.
19. S. J. Cho, J. H. Boo, J. M. Kim, D. G. Jung and S. S. Kim, *Adv. Mater. Res.*, 2011, **415-417**, 1879-1882.
20. R. S. Bedi, R. Cai, C. O'Neill, D. E. Beving, S. Foster, S. Guthrie, W. Chen and Y. Yan, *Micropor. Mesopor. Mater.*, 2012, **151**, 352-357.
21. C. O'Neill, D. E. Beving, W. Chen and Y. Yan, *Aiche J.*, 2006, **52**, 1157-1161.
22. M. Machida, K. Norimoto and T. Watanabe, *J. Mater. Sci.*, 1999, **34**, 2569-2574.
23. V. Spagnol, H. Cachet, B. Baroux and E. Sutter, *J. Phys. Chem. C*, 2009, **113**, 3793-3799.
24. K. Nakata and A. Fujishima, *J. Photoch. Photobio. C*, 2012, **13**, 169-189.
25. Y. Chang, H. Lin and C. Chen, *Electrochem. Solid St.*, 2011, **14**, 1-4.
26. A. Aladjem, *J. Mater. Sci.*, 1973, **8**, 688-704.
27. C. Chen, K. Ozasa, F. Kitamura, K. Katsumata, M. Maeda, K. Okada and N. Matsushita, *Electrochim. Acta*, 2015, **153**, 409-415.
28. J. M. Macak, H. Tsuchiya and P. Schmuki, *Angew. Chem. Int. Ed.*, 2005, **44**, 2100-2102.
29. H. Yin, H. Liu and W. Z. Shen, *Nanotechnology*, 2010, **21**, 035601-035607.
30. J. M. Macak, K. Sirotna and P. Schmuki, *Electrochim. Acta*, 2005, **50**, 3679-3684.
31. J. Yu, G. Dai and B. Cheng, *J. Phys. Chem. C*, 2010, **114**, 19378-19385.
32. S. Berger, A. Ghicov, Y. C. Nah and P. Schmuki, *Langmuir*, 2009, **25**, 4841-4844.
33. P. Acevedo-Pena, J. Vazquez-Arenas, R. Cabrera-Sierra, L. Lartundo-Rojas and I. Gonzalez, *J. Electrochem. Soc.*, 2013, **160**, C277-C284.
34. Z. Zhang, Z. Huang, X. Cheng, Q. Wang, Y. Chen, P. Dong and X. Zhang, *Appl. Surf. Sci.*, 2015, **355**, 45-51.
35. Y. Song, F. Schmidt-Stein, S. Bauer and P. Schmuki, *J. Am. Chem. Soc.*, 2009, **131**, 4230-4232.
36. B. Yu, A. Tsai, S. Tsai, K. Wong, Y. Yang, C. Chu and J. Shyue, *Nanotechnology*, 2008, **19**, 255202-255206.
37. K. Zhu, N. R. Neale, A. Miedaner and A. J. Frank, *Nano Lett.*, 2006, **7**, 69-74.

ARTICLE

RSC Advances

38. Y. Taguchi, E. Tsuji, Y. Aoki and H. Habazaki, *Appl. Surf. Sci.*, 2012, **258**, 9810-9815.
39. L. Zhang, R. Dillert, D. Bahnemann and M. Vormoor, *Energy Environ. Sci.*, 2012, **5**, 7491-7507.
40. S. Permpoon, G. Berthomé, B. Baroux, J. C. Joud and M. Langlet, *J. Mater. Sci.*, 2006, **41**, 7650-7662.

Table of Contents Entry



Durable superhydrophilic titanium plate with micro-nano composite architecture synthesized by anodization.